A novel activated carbon-supported multi-metal oxides for peroxydisulfate activation and efficient organic pollutant degradation: Insights into operations, transformation mechanism, and DFT study

Rasool Pelalak[1,2], Babak Kakavandi[3,*], Hua Yang[4,5], Parnia Bashardoust[6], Yueping Bao[7,*], Raf Dewil [8,9]

[1] Institute of Research and Development, Duy Tan University, Da Nang, Vietnam
[2] School of Engineering & Technology, Duy Tan University, Da Nang, Vietnam
[3] Department of Environmental Health Engineering, Alborz University of Medical Sciences, Karaj, Iran
[4] State Key Laboratory of Advanced Processing and Recycling of Non-ferrous Metals, Lanzhou University of Technology, Lanzhou 730050, China
[5] School of Science, Lanzhou University of Technology, Lanzhou 730050, China
[6] Department of Environmental Health Engineering, School of Public Health, Tehran University of Medical Sciences, Tehran, Iran
[7] MOE Key Laboratory of Pollution Processes and Environmental Criteria, College of Environmental Science and Engineering, Nankai University, 300350 Tianjin, China
[8] KU Leuven, Department of Chemical Engineering, Process and Environmental Technology Lab, Sint-Katelijne-Waver, Belgium
[9] University of Oxford, Department of Engineering Science, Parks Road, Oxford, OX1 3PJ, United Kingdom

*** Corresponding authors:**

Department of Environmental Health Engineering, Alborz University of Medical Sciences, Karaj, Iran. kakavandibvch@gmail.com (B. Kakavandi).

College of Environmental Science and Engineering, Nankai University, 300350 Tianjin, China. yueping.bao@nankai.edu.cn (Y. Bao).

Text S1

All chemical reagents were used without further purification. All chemicals and materials applied in this work including BPA (analytical standard, > 99%), ferric chloride hexahydrate ($FeCl_3 \cdot 6H_2O$, >98%), ferrous chloride tetrahydrate ($FeCl_2 \cdot 4H_2O$, >99%), cobalt nitrate ($Co(NO_3)_2 \cdot 6H_2O$), ferric nitrate ($Fe(NO_3)_3 \cdot 9H_2O$), technical grade persulfate ($Na_2S_2O_8$, 99%), L-Histidine (L-his), ethanol (EtOH, C_2H_5OH), peroxymonosulfate (PMS, $KHSO_5 \cdot 0.5KHSO_4 \cdot 0.5K_2SO_4$), sodium thiosulfate ($Na_2S_2O_3 \cdot 5H_2O$, 99%), tert-butyl alcohol (TBA), humic acid (HA), sodium bicarbonate ($NaHCO_3$), sodium chloride (NaCl), L-carnosine (L-car), and sodium nitrate ($NaNO_3$) were supplied from Sigma Aldrich Inc., USA. The solutions in throughout the catalyst synthesis and environmental experiments were prepared using deionized distilled water (DDW). Hydrochloric acid (HCl, 0.1 M) and sodium hydroxide (NaOH, 0.1 M) solutions were used for pH adjustment of samples. Deionized (DI) water was used in all experiments.

Text S2

A chemical co-precipitation procedure was employed for the fabrication of pure magnetite (Fe_3O_4, FO) using ferrous and ferric salts under an alkaline environment. To eliminate the dissolved oxygen, firstly, DI was purged with N_2 gas for 30 min. A solution containing ferrous chloride (0.04 M) and ferric chloride (0.06 M) was prepared and mixed for 45 min to obtain a homogeneous mixture at 70 ± 1°C. Next, the pH of the mixture was adjusted to 10.0-11.0 by dropwise adding 30 mL of 28% (w/w) ammonia solution ($NH_3^- \cdot H_2O$). After mixing for 1 h at 80 °C, a resulting black solid was obtained, collected by an external magnet, and then washed several times with DI and ethanol. The final black, solid powder of FO nanoparticles was obtained after drying overnight at 105 °C in a hot-air oven. The AC-coated magnetite nanoparticles (ACFO) composite was prepared in a similar procedure, except that a certain amount of AC was added to the solution of metal salts. Herein, two various mass ratios of AC to FO (AC:FO= 1:1 and 1:2) were synthesized to determine the best ratio of ACFO components.

For the fabrication of cobalt ferrite ($CoFe_2O_4$, CF) nanoparticles, according to the co-precipitation method, 20 mL DI containing 0.73 g $Co(NO_3)_2 \cdot 6H_2O$ and 2.02 g $Fe(NO_3)_3 \cdot 9H_2O$ (with a molar ratio of 1:2) was prepared. Thereafter, the solution pH was set above 12.0 by using NaOH (50%). After continuous stirring at 80 °C for 2 h, the black product was obtained, separated magnetically, washed with DI and ethanol several times, and then dried in a vacuum oven at 60 °C for 24 h. The ACMO composite was synthesized in a similar protocol to CF nanoparticles, with the difference that specific amounts of the prepared ACF were added to the solution of Fe and Co salts. Briefly, 100 mL of DI containing $Co(NO_3)_2 \cdot 6H_2O$ and $Fe(NO_3)_3 \cdot 9H_2O$ was prepared to achieve a metallic salt mixture. Then, specific amounts of the prepared ACFO were added to the above solution. To form a homogeneous solution, the mixture was stirred at room temperature for 30 min using a mechanical mixer. Subsequently, the mixture pH was tuned to above 12.0 by adding freshly prepared NaOH solution (50%) under constant stirring. The prepared sample was stirred for 2 h at 80 °C and then cooled down to 25 °C by further stirring. The acquired dark brown precipitates were separated magnetically and washed several times with EtOH and deionized water to remove impurities (chloride and sodium precipitates). Eventually, the obtained product was dried under a vacuum oven at 60 °C for 24 h. The CF nanoparticles were synthesized in a similar method without adding the ACFO. In this work, we

synthesized the various composites with different mass ratios of AC:FO:CF (1:1:1, 1:1:2, and 1:2:1) to obtain the best ratio of composite components.

Text S3

Powder X-ray diffraction (XRD) analysis was obtained on a Quantachrome, NOVA 2000, USA, for structure and phase characterization and crystallinity of samples using a graphite monochromatic Cu Kα radiation for 2θ scanning range between 10° and 80° with the scan rate of 10°/min. Besides, the average crystallite size of the samples was calculated by the Debye-Scherrer formula. The prepared samples (i.e., CF, ACFO and ACMO) were instrumentally analyzed by using Brunaeur, Emmett and Teller (BET, Quantachrome, NOVA 2000, USA) to characterize the size and volume of pores, the specific surface area and textural properties, transmission electron microscope (TEM, PHILIPS, EM, Netherlands) for size and shape analysis of particles, scanning electron microscope SEM (SEM/JSM-6700F) equipped an energy dispersive X-ray spectrometer (EDS) for characterization of the external morphology, internal structure and elemental and vibrating sample magnetometer (VSM, 7400, Lakeshore, USA) for magnetic properties. To investigate the change properties of the ACMO composite, its zeta potential was measured by using Zetasizer Nano ZS90 (UK) in an aqueous solution with a range of pH values (1.0-12.0).

Text S4

The residual concentrations of BPA were measured using an HPLC (Agilent 1200 Infinity Series, USA) instrument equipped with a C18 column (100–5; 4.6 mm× 250 mm, 5 μm), using a detector at a wavelength of 214 nm. The mobile phases were a mixture of ultrapure water and acetonitrile in the volume ratios of 50 v:50 v and used with the flow rate of 1 mL/min. An inductively coupled plasma mass spectrometry (ICP-MS, Thermo Fisher Scientific iCAP Q, USA) was used for the measurement of the contents of metal ions (Fe and Co) leached from the catalyst to estimate the catalyst durability. The mineralization degree was determined using a measure of total organic carbon (TOC) concentrations of samples by a TOC analyzer (TOC-L CPH, Shimadzu, Kyoto, Japan). The formed intermediate products during the BPA degradation were identified by using an HPLC-MS (Shimadzu, Japan) as follows: Acetonitrile solution containing 0.1 % formic acid and water containing 0.1 % formic acid were used as the mobile phases with a flow rate of 0.8 mL/min.

Table S1.
The results are related to the BET analysis for the materials used in this study.

Samples	S_{BET} (m^2/g)	Total pore volume (cm^3/g)	Average pore diameter (nm)	Pore structure
AC	1228	0.695	2.35	Mesopore
ACF	498.06	0.382	2.96	Mesopore
ACMO	330.2	0.239	2.89	Mesopore

Table S2.

Comparisons of the PS-oxidation performance of ACMO with those of reported catalysts to degrade BPA.

Catalyst/system	Experimental conditions	Degradation efficacy (%)	TOC removal (%)	$k_{obs}\times10^{-3}$ (min^{-1})	Ref.
Fe-Cu@carbon + PS	pH: 5.0 Catalyst: 1.0 g/L PS: 0.028 μM BPA: 50 mg/L	100 (10 min)	76 (after 60 min)	-	[1]
$Ni_{0.60}Co_{0.40}O_x$ NSs + PS	pH: 7.9 Catalyst: 0.1 g/L PS: 75 μM BPA: 10 mg/L	100 (25 min)	28.3	0.232	[2]
Fe-Cu/PS	pH: 6.2 Catalyst: 0.15 g/L PS: 0.6 mM BPA: 20 mg/L	99 (60 min)	72.32	0.215	[3]
CuO/MSS/PS	pH: 3-9 Catalyst: 1.5 g/L PS: 100 mM BPA: 50 mg/L	92 (45 min)	80	0.14	[4]
$LaFeO_3$/GO/PS	pH: Natural Catalyst: 0.5 g/L PS: 2.0 mM BPA: 20 mg/L	97 (90 min)	51	0.1074	[5]
Fe_3O_4@MBC800/PS	pH: 6.62 Catalyst: 0.5 g/L PS: 5.0 mM BPA: 20 mg/L	96.73 (180 min)	-	0.019	[6]
Mn_2O_3/Mn_3O_4-$Cu_{1.5}Mn_{1.5}O_4$/PS	pH: 6.3 Catalyst: 0.2 g/L PS: 2.0 mM BPA: 10 mg/L	98.3 (120 min)	66.2	0.0489	[7]

PSBC950/PS	pH: without adjustment Catalyst: 0.4 g/L PS: 5.0 mM BPA: 0.088 mM	98.24 (60 min)	-	0.0845	[8]
FeCo-NC600/PS	pH: 7.0 Catalyst: 0.1 g/L PS: 0.5 mM BPA: 50 μM	100 (20 min)	85	0.2876	[9]
Fe-Cu@carbon/PS	pH: 5.0 Catalyst: 1.0 g/L PS: 0.028 mM BPA: 50 mg/L	95 (30 min)	76	-	[1]
ACMO/PS	pH: 6.0 Catalyst: 0.2 g/L PS: 3.0 mM BPA: 20 mg/L	100 (60 min)	72.6	0.214	This study

Fig. S1:

Zeta potential of the ACMO catalyst.

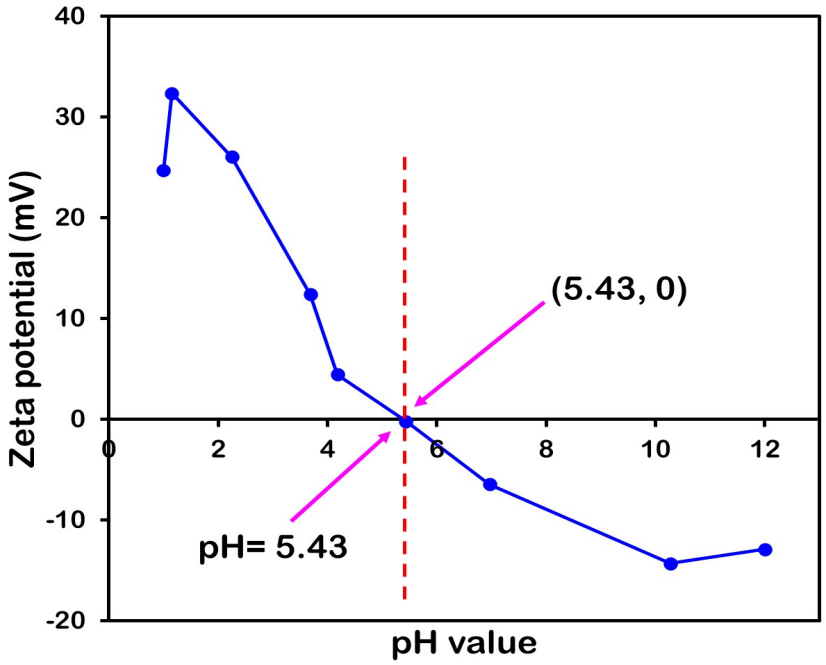

Table S3.

Characterizations of used real samples.

Parameters	values		
	STWW	River water	Tap water
pH	7.7±0.3	8.4±0.1	7.5±0.2
Chemical oxygen demand (mg/L)	158±10	16±5	ND
Total dissolved solids (mg/L)	857±4	622	465
Turbidity (NTU)	7.8±0.2	6.8	4.2±0.1
Cl^- (mg/L)	1354.8	1354.8	282.5
Sulfate (SO_4^{2-})(mg/L)	89	56	47
NO_3^- (mg/L)	121.6	121.6	56.8
PO_4^{3-} (mg/L)	137.3	28.7	ND

Table S4.

The Fukui functions of the atoms in the BPA molecule were calculated using Gaussian software at the PBE0/6-311G level of theory.

Atom	Number	f^+	f^0	f^-
O	1	0.0226	0.0454	0.0683
O	2	0.0226	0.0454	0.0683
C	3	-0.0041	0.0149	-0.0256
C	4	-0.0217	0.0393	0.1003
C	5	-0.0217	0.0393	0.1003
C	6	-0.0033	0.0011	0.0011
C	7	-0.0033	0.0011	0.0011
C	8	0.0897	0.0602	0.0307
C	9	0.0897	0.0602	0.0307
C	10	0.0876	0.0445	0.0013
C	11	0.0876	0.0445	0.0013
C	12	0.0941	0.0537	0.0132

C	13	0.0941	0.0537	0.0132
C	14	0.1009	0.0835	0.0662
C	15	0.1009	0.0835	0.0662
C	16	-0.0062	0.0337	0.0735
C	17	-0.0062	0.0337	0.0735
H	18	0.0153	0.0196	0.0239
H	19	0.0153	0.0196	0.0239
H	20	0.0145	0.0153	0.0162
H	21	0.0144	0.017	0.0196
H	22	0.003	0.0046	0.0061
H	23	0.003	0.0046	0.0061
H	24	0.0144	0.017	0.0196
H	25	0.0145	0.0153	0.0162
H	26	0.0119	0.013	0.0141
H	27	0.0119	0.013	0.0141
H	28	0.0228	0.0235	0.0242
H	29	0.0228	0.0235	0.0242
H	30	0.0272	0.0272	0.0271
H	31	0.0272	0.0272	0.0271
H	32	0.0294	0.0282	0.0271
H	33	0.0294	0.0282	0.0271

Table S5.
The intermediate products were identified by LC-MS.

No.	Compound name	m/z	Molecular formula	Tentative structure
-	BPA	227	$C_{15}H_{16}O_2$	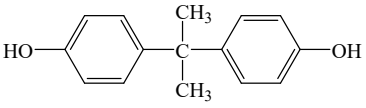
P1	Monohydroxylated BPA	243	$C_{15}H_{16}O_3$	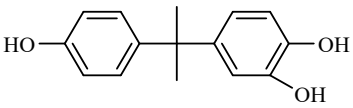
P2	Dihydroxylated BPA	259	$C_{15}H_{16}O_4$	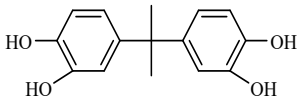
P3	Quinone of dihydroxylated BPA	256	$C_{15}H_{14}O_4$	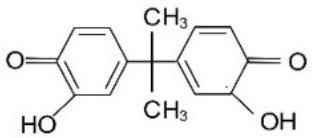
P4	(2E,4Z)-3-(2-(3,4-dioxocyclohexa-1,5-dien-1-yl)propan-2-yl) hexa-2,4-dienedioic acid)	289	$C_{15}H_{14}O_6$	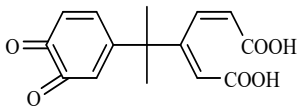
P5	4,5-Bisphenol-o-quinone	241	$C_{15}H_{14}O_3$	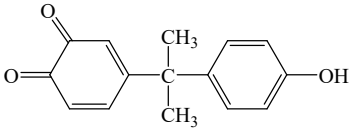
P6	4-(2,3-dimethylbut-3-en-2-yl)phenol	175	$C_{12}H_{16}O$	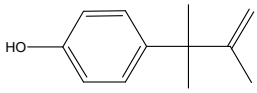
P7	4-hydroxyacetophenone	135	$C_8H_8O_2$	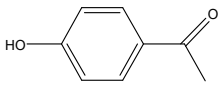
P8	phenol	93	C_6H_6O	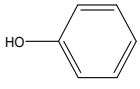

P9	hydroquinone	110	$C_6H_6O_2$	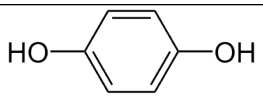
P10	p-benzoquinone	108	$C_6H_4O_2$	

References:

[1] A. Están García, N. Crespí Sánchez, G. Turnes Palomino, C. Palomino Cabello, MOF derived porous Fe-Cu@carbon catalyst for the degradation of bisphenol A through a persulfate-based advanced oxidation process, Microporous and Mesoporous Materials 381 (2025) 113366.

[2] M.-M. Wang, P.-X. Liu, F. Ye, L.-J. Liu, J.-T. Wen, B.-J. Ni, H.-W. Luo, W.-K. Wang, J. Xu, 2D Ni-Co bimetallic oxide nanosheets activate persulfate for targeted conversion of bisphenol A in wastewater into polymers, Environment International 184 (2024) 108466.

[3] Z. Tang, W. Yu, W. Wu, L. Zhu, Y. Ye, C. Gao, B. Wang, S. Ren, Preparation of Fe-Cu bimetal from copper slag by carbothermic reduction–magnetic process for activating persulfate to degrade bisphenol A, Journal of the Taiwan Institute of Chemical Engineers 146 (2023) 104784.

[4] S. Liang, Z. Ziyu, W. Fulong, B. Maojuan, D. Xiaoyan, W. Lingyun, Activation of persulfate by mesoporous silica spheres-doping CuO for bisphenol A removal, Environmental Research 205 (2022) 112529.

[5] J. Jing, C. Cao, S. Ma, Z. Li, G. Qu, B. Xie, W. Jin, Y. Zhao, Enhanced defect oxygen of $LaFeO_3$/GO hybrids in promoting persulfate activation for selective and efficient elimination of bisphenol A in food wastewater, Chemical Engineering Journal 407 (2021) 126890.

[6] Y. Yu, H. Guo, Z. Zhong, A. Wang, M. Xiang, S. Xu, C. Dong, Z. Chang, Fe_3O_4 loaded on ball milling biochar enhanced bisphenol a removal by activating persulfate: Performance and activating mechanism, Journal of Environmental Management 319 (2022) 115661.

[7] Y. Zhu, Z. Sun, Y. Deng, F. Liu, W. Ruan, L. Xie, Mn_2O_3/Mn_3O_4-$Cu_{1.5}Mn_{1.5}O_4$ spinel as an efficient Fenton-like catalyst activating persulfate for the degradation of bisphenol A: Superoxide radicals dominate the reaction, Science of The Total Environment 839 (2022) 156075.

[8] Z.-J. Wang, Y.-Q. Lin, H.-J. Zhou, Z.-L. Liu, R.-R. Miao, X.-M. Xu, L. He, Q.-Q. Guan, Boosting persulfate activation via paper mill sludge-based biochar for efficient degradation of bisphenol A: Inherent multiple active sites, Chemical Engineering Journal 455 (2023) 140795.

[9] Y. Wang, C.-Y. Gao, Y.-Z. Zhang, M.K.H. Leung, J.-W. Liu, S.-Z. Huang, G.-L. Liu, J.-F. Li, H.-Z. Zhao, Bimetal-organic framework derived CoFe/NC porous hybrid nanorods as high-performance persulfate activators for bisphenol a degradation, Chemical Engineering Journal 421 (2021) 127800.